ELSEVIER

Contents lists available at ScienceDirect

# Journal of Colloid And Interface Science

journal homepage: www.elsevier.com/locate/jcis



#### **Short Communication**

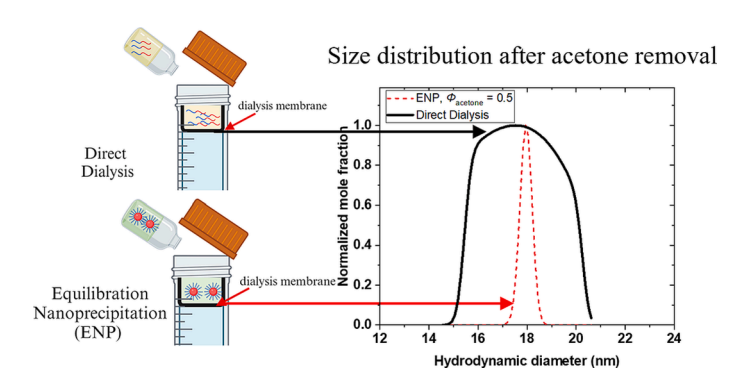


# Overcoming limitations of conventional solvent exchange methods: Achieving monodisperse non-equilibrium polymer micelles through equilibration-nanoprecipitation (ENP)

Daniel J. Fesenmeier<sup>a</sup>, Elliot S. Cooper<sup>a</sup>, You-Yeon Won<sup>a,b,\*</sup>

- <sup>a</sup> Davidson School of Chemical Engineering, Purdue University, West Lafayette, IN 47907, USA
- <sup>b</sup> Purdue University Institute for Cancer Research, West Lafayette, IN 47907, USA

#### GRAPHICAL ABSTRACT



#### ARTICLE INFO

# Keywords: Poly(styrene)-poly(ethylene glycol) Block copolymer micelles Kinetically frozen micelles Non-equilibrium micelles Solvent exchange Equilibration-nanoprecipitation

#### ABSTRACT

#### Hypothesis

Conventional solvent exchange formulation methods face limitations when trying to control the final non-equilibrium size properties of block copolymer micelles containing a strongly hydrophobicity and a rigid block because the solvent conditions are not well controlled during micelle formation. Therefore, using an alternative formulation method, named Equilibration-Nanoprecipitation (ENP), in which micelles are formed under uniform solvent conditions, will significantly reduce the final dispersity compared a conventional solvent exchange method.

*Experimental:* Size properties of the final aqueous micelle dispersions formed from the ENP method and a conventional solvent exchange are measured using DLS. Also, a parallel modelling study is completed to predict the final size distributions using both methods.

#### Findings

The experimental results demonstrate the ENP method is effective producing non-equilibrium micelles with low dispersity below the monodisperse polydispersity index (*PDI*) cutoff for DLS while the conventional solvent exchange method leads to significantly greater dispersity. Also the experimental results highlight ENP can be used to tune the final size properties which cannot be done using methods which do not properly control the

<sup>\*</sup> Corresponding author at: Davidson School of Chemical Engineering, Purdue University, West Lafayette, IN 47907, USA. *E-mail address:* yywon@purdue.edu (Y.-Y. Won).

micelle formation conditions. Additionally, the modelling study supports the utility of the ENP approach for producing monodisperse dispersions of nonequilibrium polymer micelles.

#### 1. Introduction

The self-assembly of amphiphilic block copolymers (BCPs) in aqueous conditions has been extensively studied over the past several decades due to their promising use in applications such as surfactants and drug delivery agents [1]. The self-assembly characteristics of BCPs depend on a variety of factors. BCPs with not too strongly hydrophobic blocks (e.g., Pluronic surfactants from BASF) can be directly dissolved in aqueous conditions [2,3]. Self-assembly will then occur once a sufficiently high concentration, known as the critical micelle concentration (CMC), is reached [4]. However, for BCPs with strongly hydrophobic blocks with high glass transition temperature  $(T_{\sigma})$  values (e.g., poly (styrene) (PS)), direct molecular dissolution of the polymer is not possible [5,6]. To circumvent the insolubility of the hydrophobic block in water, several methods are conventionally used to study the selfassembly properties of these systems. These methods, commonly referred to as solvent exchange methods, involve initially dissolving the polymer in a non-aqueous common solvent ("co-solvent") which is compatible with both blocks [7]. Then, the solvent conditions are exchanged from co-solvent-rich to water-rich by slowly adding water while mixing, directly dialyzing against water, or by introducing the cosolvent solution into a large water reservoir. Finally, dialysis or evaporation/distillation can be used to completely remove the co-solvent. These conventional solvent exchange methods, however, face limitations when seeking to scale up the production of monodisperse micelles of a BCP system with a strongly hydrophobic block with a high  $T_g$ .

When producing aqueous micelle suspensions using BCP materials with highly hydrophobic and rigid core-forming blocks, the final self-assembled structures are non-equilibrium in nature [8]. Since the structures are no longer equilibrium micelles, they are commonly referred to as kinetically frozen or kinetically trapped micelles or nanoparticles [9]. In contrast, small molecule surfactants and Pluronic surfactants form equilibrium micelles in water and the final structures depend on thermodynamic conditions, including the chemical characteristics of the surfactants, temperature, ion content, etc. [10,11]. In this manuscript, the term micelle will be used to imply a self-assembled corecorona polymer structure and is not meant to imply that the micelle is in dynamic equilibrium. The non-equilibrium quality implies that the final structure will change depending on the formulation pathway [12,13]. Because the final structures are non-equilibrium, the formulation pathway must be carefully designed to control the final size properties.

When considering the self-assembly of a BCP system with a fixed molecular weight in a water/organic solvent mixture, the self-assembly is controlled by the interfacial tension between the hydrophobic block and the solvent [14]. In the range of water content where equilibrium structures are formed, the equilibrium aggregation number will increase with increasing water volume fraction. Therefore, to control the final non-equilibrium size properties, the solvent conditions must be carefully changed in order to ensure the entire micelle population is formed under the same conditions. Because conventional solvent exchange methods induce micellization under conditions of constantly changing solvent conditions, they do not lend themselves well to properly controlling the final size properties. To examine this point, in this manuscript we compare the final size properties of micelles formed from a conventional solvent exchange method with those obtained through a method, referred to as "Equilibration-Nanoprecipitation" or "ENP", which is designed to strategically control the solvent conditions during micelle formation [15]. The ENP formulation method has become the method of choice of the Polymer Lung Surfactant (PLS) technology being developed in our group for which the size properties significantly affect the critical quality attributes of the PLS formulation [16].

The ENP method is designed to control the final size and dispersity of the aqueous micelle system in the following manner. First, the micellization is initiated by directly adding the polymers to a water/acetone mixture at solvent compositions where equilibrium is possible. Next, the solution is kept stirring overnight to allow for the micelle structures to equilibrate under the uniform solvent conditions. Lastly, dialysis is used to quickly change the solvent content to the water-rich state where dynamic rearrangement is not possible. The size properties are measured using dynamic light scattering (DLS) and the results are compared between the ENP method and the solvent exchange method. The polymer material used is poly(styrene)(5.2 kDa)-b-poly(ethylene glycol)(5.5 kDa) (PS-PEG) which has been identified as a promising candidate for the PLS application [17–20]. Given the application of the formulated polymer micelles, surface mechanical properties of batches formed using ENP and solvent exchange are compared. Lastly, a computational approach is used to predict the effect of formulation method on the final size distributions. The experimental and computational results both highlight the importance of controlling micelle formation conditions on reproducibly producing non-equilibrium polymer micelles with controlled size and dispersity.

#### 2. Methods/procedures

#### 2.1. Polymer materials

Poly(styrene)(5.2 kDa)-b-poly(ethylene glycol)(5.5 kDa) (PS-PEG) was purchased from Polymer Source, Inc., with the molecular weight values provided in parentheses denoting the number-average molecular weights of the respective blocks. According to the vendor, this BCP was synthesized via anionic polymerization and includes a hydroxyl functionality at the terminus of the PEG block.

#### 2.2. Polymer characterization

The overall molecular weight polydispersity index was determined to be 1.11 through gel permeation chromatography (GPC) using a Waters 1515 isocratic pump fitted with Styragel HR 4 and Ultrastyragel columns. The mobile phase employed was THF, with a flow rate of 1 mL/min. Calibration was performed using polystyrene standards, and the chromatograph can be observed in Figure S1 in the Supporting Material (SM).

#### 2.3. Equilibration-Nanoprecipitation (ENP) micelle formulation method

PS-PEG (10 mg) is dissolved in a 2 mL mixture of acetone (Sigma-Aldrich) and Milli-Q-purified water (18  $M\Omega\text{-cm}$  resistivity) under sonication. The solution is then repeatedly vortexed and sonicated until the solution appears transparent. The solution is then stored under gentle rocking at room temperature for 24 h to allow for equilibration. Acetone is then removed by dialyzing the 2 mL mixture (initially containing  $\sim\!\!1$  mL of acetone) using Slide-A-Lyzer Mini Dialysis device (20 kDa MWCO, Thermo Fisher Scientific) against Milli-Q-purified water for 24 h (following the manufacturer's recommendation), replacing the water reservoir at 1, 2, 4 and 6 h time points. The water reservoir is 45 mL. The anticipated acetone content in the final micelle solution is expected to be  $<\!\!1$  ppm.

#### 2.4. Direct dialysis micelle formulation method

The procedure is the same as for the ENP procedure except that the polymer is dissolved into acetone only and not an acetone/water

mixture.

#### 2.5. Surface pressure-area (SPA) isotherms

The surface pressure-area isotherms are measured using a KSV Nima Langmuir trough (51 cm  $\times$  14.5 cm) with double symmetric barriers. The total surface area of the trough is 780 cm², and the subphase volume is 750 mL. A filter paper probe is used for surface tension measurements. Micelle samples are spread onto water using a Hamilton microsyringe at a concentration of 5 mg/mL. The compressions are done at a rate of 3 mm/minute. The temperature of the subphase is held constant at 25  $^{\circ}\text{C}$  using a circulating water bath.

#### 2.6. Polymer micelle characterizations

The hydrodynamic diameters of the block copolymer micelles are measured at 25 °C by dynamic light scattering (DLS) using a Brookhaven ZetaPALS instrument. The scattering intensities are measured using a 659 nm laser at a scattering angle of 90°. The hydrodynamic diameters ( $D_h$ ) were calculated from the measured diffusion coefficients ( $D_t$ ) using the Stokes-Einstein equation ( $D_h = \frac{k_B T}{3\pi\eta_o D_t}$  where T is temperature,  $k_B$  is Boltzman's constant, and  $\eta_o$  is the viscosity of the medium). The results were averaged over 5 runs. The samples were diluted to 1 mg/mL and filtered using 450 nm syringe filters to remove any particulates. Transmission electron microscopy (TEM) images of micelles formed by the same polymer using the ENP method were presented in our prior publication [16].

#### 2.7. Modelling approach for predicting size distribution of micelles

A computational approach was utilized to predict the distribution of size characteristics for polymer micelles formed by ENP or the traditional direct dialysis procedure for co-solvent removal. The approach is an extension of the work by R. Nagarajan [8,14] who developed a phenomenological theory to a priori predict micelle size characteristics for "non-equilibrium" micelles. The approach uses a free energy minimization to first determine the "equilibrium" size of the micelles; equilibrium micelles can be formed when the selective solvent (water) is less than the critical water volume fraction (the water volume fraction at which the core becomes glassy). Above the critical water fraction, the aggregation number is fixed because free exchange of chains is not possible. To determine the final size, the free energy minimization is recalculated with a fixed aggregation number. Finally, a Gibbs (Boltzmann) distribution is applied to predict the distribution of micelle sizes under different formulation conditions. A complete description of the computational approach is given in the SM.

#### 3. Results and discussion

#### 3.1. Experimental results

To examine the effect of formulation method on the final size distribution, size reproducibility, and final material properties, PS-PEG micelles were formulated using two different methods: direct dialysis, an example of a conventional solvent exchange formulation method, and ENP, the established method for formulating Polymer Lung Surfactant (PLS) materials [16–18]. The schematic of the methods is shown in

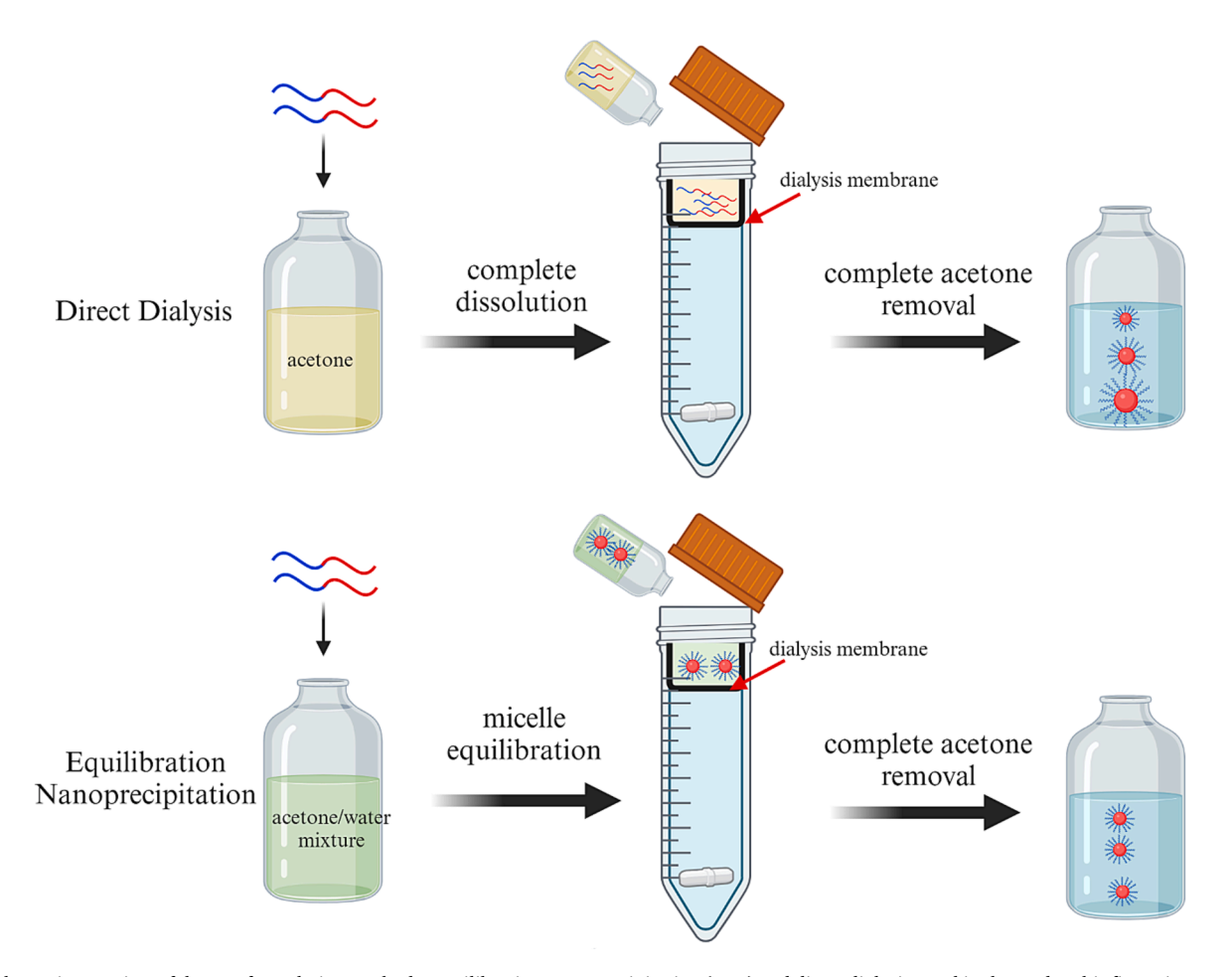


Fig. 1. Schematic overview of the two formulation methods, Equilibration-Nanoprecipitation (ENP) and direct dialysis, used in the study. This figure is reproduced in color on the web and in black-and-white in print.

Fig. 1. The difference between the two protocols is that for ENP, the polymer chains are added directly to an acetone/water mixture which induces polymer self-assembly under a uniform solvent condition. Dialysis is then utilized to quickly increase the water content with the goal of preserving the original equilibrium size distribution. For direct dialysis, polymers are dissolved in pure acetone which does lead to self-assembly because acetone is a good solvent for both blocks. Therefore, the self-assembly is induced during the dialysis step. Because of solvent gradients which are inherent in the dialysis process, the final size distribution is expected to have a relatively higher dispersity compared to ENP.

To examine the difference in final size distribution and batch-tobatch reproducibility, DLS was employed to measure the mean hydrodynamic diameter ( $D_h$ , defined as the intensity-weighted Z-average mean size  $(Z_D)$  using cumulants analysis), polydispersity index (PDI,defined as  $\frac{\sigma^2}{Z^2}$  in the cumulants analysis where  $\sigma$  is the standard deviation of the distribution), and size histograms (calculated based on nonnegatively constrained least-squares (NNLS) inversion method) using three separate batches from each formulation method. For the reproducibility study, the initial volume fraction of acetone for ENP samples was of  $\Phi_{acetone} = 0.70$ . The average and standard deviation (SD) values for  $D_h$  and PDI from cumulants analysis in three independent batches are shown in Table 1 and the DLS size distribution histograms are shown in Fig. 2. The results indicate that the ENP method reproducibly results in lower dispersity across the three batches, which is indicated qualitatively by the narrower peaks around 30 nm in the histogram plots and quantitatively by the PDI/CV values in Table 1. Typically for DLS, samples with a *PDI* of < 0.1 are considered monodisperse, and the results suggest ENP is capable of meeting this criteria.

The effect of ENP formulation condition on the final distribution was also evaluated. The  $D_h$  and PDI of ENP formulation conditions ranging from  $\Phi_{acetone}=0.40$  to  $\Phi_{acetone}=0.80$  are included in Table 2, and the size distributions are shown Figure S2 in the SM. The results demonstrate that the  $D_h$  increases with decreasing ENP formulation  $\Phi_{acetone}$ values, which shows the effect of the formulation solvent interfacial tension on the final size properties. The PDI and distribution results indicate that at both the low (0.4) and high (0.8) ends of the  $\Phi_{acetone}$ range, the ENP is less effective at producing monodisperse final populations. It is likely that at high (  $\geq$  0.8)  $\varPhi_{\textit{acetone}}$  values, the formulation becomes more similar to direct dialysis whereby dynamic rearrangement is more favorable at higher acetone contents and the final micelle structures are formed under a solvent gradient during the dialysis process. In contrast, at low ( $\leq$  0.4)  $\Phi_{acetone}$  values, the formation of larger non-equilibrium aggregates can occur during formulation due to the high interfacial tension between the core block and water, which requires vigorous mixing for extended time periods to fully disassociate.

Our group is particularly interested in the formulation of PS-PEG kinetically trapped micelles in water due to their promising application as a lung surface replacement therapy [17,18]. The efficacy of a lung surfactant replacement therapy is directly related to its surface mechanical behavior. More specifically, its ability to lower the high air—water interfacial tension is critical to stabilize the alveoli and allow for proper respiratory function. The surface tension lowering properties are studied using a Langmuir trough Wilhelmy plate setup whereby the micelles are spread onto the water surface, where they rapidly adsorb to

**Table 1** DLS results in terms of mean hydrodynamic diameter  $(D_h)$  and polydispersity index (PDI) for micelles produced using the two different formulation methods after acetone removal. Each value represents the average and standard deviation of three different batches. The coefficient of variance (CV) is calculated from the square root of the PDI from DLS  $(CV = PDI^{1/2})$ .

Formulation Method	D <sub>h</sub> (nm)	PDI	CV
Direct Dialysis	$33.3 \pm 1.6$	$0.214 \pm 0.006$	0.463
ENP, $\Phi_{acetone} = 0.70$	$28.7 \pm 0.6$	$0.096 \pm 0.022$	0.309

the interface, and two symmetric barriers are used to compress the film. The change in surface tension is measured as a function of trough area. Based on the same rationale applied to poly(butadiene)-poly(ethylene glycol) (PB-PEG) [21], it is expected that the 5.2 kDa-5.5 kDa PS-PEG material is entirely insoluble in water, leading to an effectively zero critical micellization concentration (CMC). Consequently, water-spread PS-PEG micelles will retain their original micelle morphology at the interface, akin to what has been observed with water-spread poly(lacticco-glycolic acid)-poly(ethylene glycol) micelles [22]. Additionally, our recent studies [23-25] have demonstrated that the core domains of PS-PEG micelles exist in a frozen (glassy) state at room temperature. Therefore, despite the use of the term "micelle", it is more accurate to consider PS-PEG micelles as PEG-brushed solid nanoparticles. These PS-PEG micelle structures do not dissociate into free chains and are incapable of undergoing morphological rearrangements. Furthermore, the PS-PEG micelles are thought to be strongly anchored to the interface due to the highly hydrophobic PS domain, which is what allows the production of very low surface tension (very high surface pressure) during compression [20]. If the micelles were to readily desorb into the subphase, there would not be a rapid reduction of surface tension during compression. For the same reason, there is typically no significant loss of micelles to the subphase during the initial spreading, provided that an excessive amount of micelles is not spread onto the water surface [20].

The effect of formulation method on the corresponding surface mechanical behavior of the micelle solutions was evaluated by measuring surface pressure-area (SPA) isotherms for each sample. The isotherms, shown in Fig. 3, measure the surface pressure  $(\Pi = \gamma_0 - \gamma)$  as a function of surface concentration where  $\gamma_0$  is the surface tension of the clean air-water interface and  $\gamma$  is the surface tension of the micelle-coated interface. The results demonstrate that the batches using the ENP method show much more consistent surface mechanical behavior compared to the direct dialysis method. The ENP samples display the important feature of producing high surface pressure as the monolayers collapse at surface pressures in the range of 65 - 68 mN/m; generating surface pressure greater than 60 mN/m is critical for the lung surfactant application [18]. The samples from direct dialysis method, however, show more varied surface mechanical behavior and collapse at surface pressures in the range of 53 - 60 mN/m. The effect of size properties on the surface mechanical behavior is also shown in Figure S3 in the SM which shows SPA isotherms for different ENP conditions. Given the therapeutic efficacy of the PLS is directly linked to its surface mechanical behavior, the batch-to-batch reproducibility of the SPA isotherms is deemed as a measure of quality control. Therefore, ENP is much more effective at improving quality control as demonstrated by the reproducibility of SPA isotherms.

#### 3.2. Computational results

Conceptually, the ENP method is more effective at producing monodisperse and well-controlled populations of polymer micelles because the micelles are formed under uniform/equilibrium conditions; in this limit, the sole contribution to size polydispersity is thermal fluctuation. In contrast, the conventional methods form micelles under a solvent gradient. To further examine the effect of formulation conditions on the final size distributions, a computational approach was used to calculate the corresponding size distributions using ENP (no solvent gradient) and direct dialysis (solvent gradient). The computational approach is an extension of the phenomenological free energy model proposed by R. Nagarajan in two prior publications [8,14] and is applied to the polymer material and solvent system used in the experimental studies in this manuscript. Specifically, this work applies the free energy minimization routine for non-equilibrium micelles to directly calculate the size distribution of micelles. Therefore, this work gives new insights into how formulation conditions affect the final size distribution/dispersity of non-equilibrium micelles.

For ENP, the computational algorithm estimates the equilibrium size

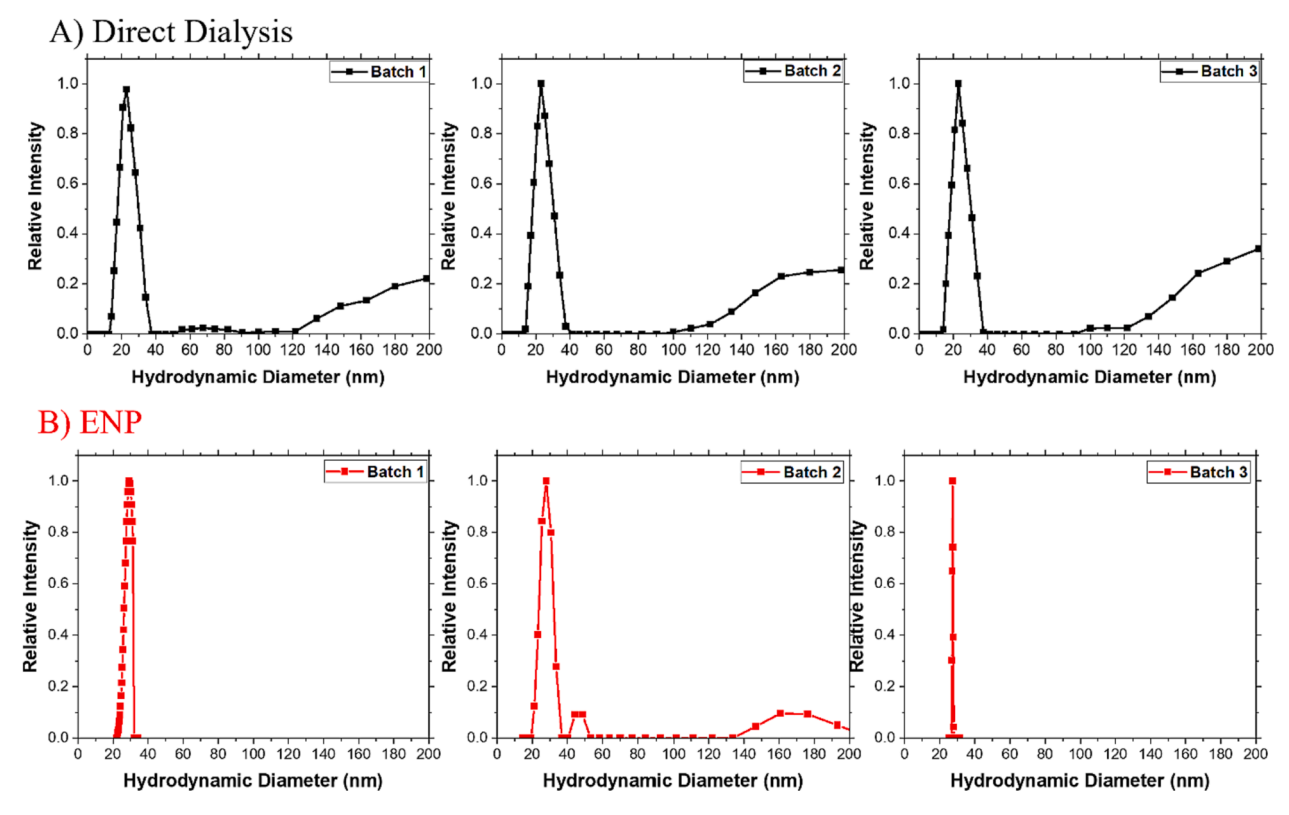


Fig. 2. DLS size distribution histograms for three batches prepared using A) direct dialysis and B) ENP,  $\Phi_{acetone} = 0.70$ . This figure is reproduced in color on the web and in black-and-white in print.

Table 2 Mean, standard deviation (SD), and coefficient of variance (CV = SD/mean) of  $D_h$  from Gaussian fits to size distribution profiles for selected ENP cases and direct dialysis. The theoretical values were estimated from the results shown in Fig. 6. The experimental values were extracted from the DLS data using cumulant analysis.

Formulation method	Mean (nm) (Theory)	SD (nm) (Theory)	CV (Theory)	Mean (nm) (Experiment)	CV (Experiment)
ENP, $\Phi_{acetone} = 0.20$	20.0	0.23	0.012		
ENP, $\Phi_{acetone} = 0.40$	18.6	0.24	0.013	52.7	0.403
ENP, $\Phi_{acetone} = 0.50$	18.0	0.25	0.014	32.8	0.202
ENP, $\Phi_{acetone} = 0.60$	17.3	0.25	0.014	29.6	0.228
ENP, $\Phi_{acetone} = 0.70$	16.7	0.25	0.015	28.7	0.309
ENP, $\Phi_{acetone} = 0.80$	16.0	0.24	0.015	28.1	0.494
Direct Dialysis ( $\Phi_{acetone} = 1$ )	17.5	2.1	0.120	33.3	0.463

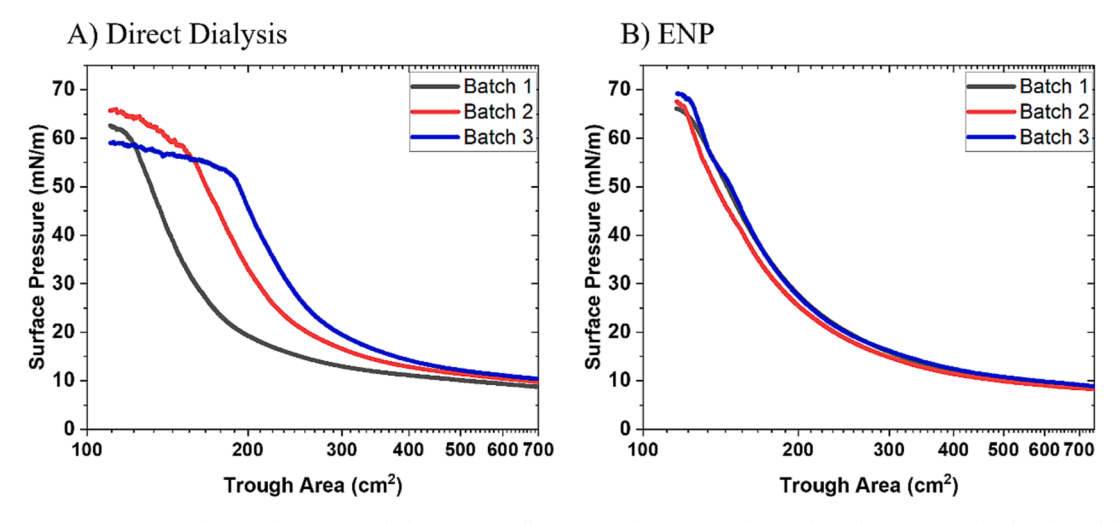


Fig. 3. Surface pressure-area (SPA) isotherms of water-spread of PS-PEG micelles (100  $\mu$ L of 5 mg/mL solution) from three separate batches formed from either direct dialysis or ENP. The isotherms were collected at 25 °C using a compression rate of 3 mm/min. This figure is reproduced in color on the web and in black-and-white in print.

distributions for micelles formed from the polymer PS(5.2 kDa)-PEG (5.0 kDa) in acetone/water mixtures at different bulk volume fractions of acetone ( $\Phi_{acetone}$ ). The algorithm, described in more detail in the SM implements a minimization of the free energy change of micelle formation using the fraction of acetone in the core ( $\eta$ ), core radius (R), and corona thickness (R) as model variables. The theory predicts that the lower  $\Phi_{acetone}$  limit for equilibrium micelle formation is set by when the free energy change of micelle formation first becomes negative. The upper  $\Phi_{acetone}$  limit is determined by Eqs. (S1), (S2), and (S3) in the SM which estimates the volume fraction of acetone in the core,  $\Phi_{crit}$ , at which the core becomes glassy at room temperature. Above  $\Phi_{crit}$  the micelle cores are 'frozen' which prevents further rearrangement and thus micelles are non-equilibrium micelles.

The complete removal of acetone from the core (which was done by dialysis in the experimental ENP procedure) produces non-equilibrium micelles due to the solid nature of the core domain. To estimate the final size properties of non-equilibrium micelles in water, the minimization was recalculated to find the final R and D values while fixing the aggregation number (g) and setting  $\Phi_{acetone}=0$ . This calculation assumes that the acetone is removed quickly such that the micelles do not have sufficient time to rearrange before the core becomes glassy. The results for the micelle radius and thickness for non-equilibrium micelles as a function of the bulk volume fraction of acetone at which they were formed are shown in Figure S4 in the SM for comparison against the size characteristics of the equilibrium micelles, where it is noted that the non-equilibrium micelles demonstrate smaller size characteristics than the equilibrium micelles due to acetone being removed from the core.

The next step of the computational approach was to determine the final size distribution (after acetone removal) of micelles for each of the solvent conditions at which equilibrium micelles were formed. This was done by using Eq. (S15) in the SM which calculates the mole fraction of micelles of aggregation number  $g(X_g)$ . To determine the mole fraction distribution, the minimization of the free energy change of polymer aggregation ( $\Delta G$ ) was calculated for a range of aggregation numbers at

various bulk solvent compositions. In this case, since the aggregation numbers were fixed, only two variables (R and D) were used in the minimization routine. This minimization provides the value for the free energy change of a polymer transitioning from the single dispersed state to a micelle of size g containing j acetone molecules ( $\Delta \mu_{gi}^{o}$ ), a parameter employed in Eq. (S15). Once the mole fractions were calculated as a function of aggregation number, the aggregation numbers were converted to final micelle size after acetone removal (i = 0) by running the minimization routine for each g value setting  $\Phi_{acetone} = 0$  and using R and D as variables. The hydrodynamic diameter is then estimated by  $D_h =$ 2R + 2D. The resulting mole fraction distribution for each of the ENP cases can be approximated well by a Gaussian distribution which allows for a direct fit of the mean and standard deviation. An example of the calculated raw data for the mole fraction of micelles alongside the Gaussian fit for the 50 % acetone/50 % water condition is shown in Fig. 4. The  $D_h$  which gives the maximum number fraction corresponds to the aggregation number which gives the minimum value for the free energy change of micellization at the given ENP formulation solvent composition condition.

In contrast to the ENP method, in the direct dialysis method the micelles are formed under a solvent composition gradient instead of one single solvent condition. To estimate the distribution for direct dialysis case, the solvent composition was assumed to vary linearly with distance away from the membrane as depicted in Fig. 5. Therefore, the distribution was estimated by summing up the mole fraction distributions for solvent conditions at which micellization occurs ( $\Phi_{acetone}=0.18-0.88$ ). For the analysis, solvent composition increments of 0.01 were used. The number of moles of the system was assumed to be uniform throughout the entire solution. The mole fraction distribution was calculated by summing up the mole fractions at a given aggregation number/size for the entire set of solvent compositions and then normalizing the distribution.

The theoretical normalized size distributions for the various ENP cases (shown in Fig. 6) provide interesting comparison to experimental

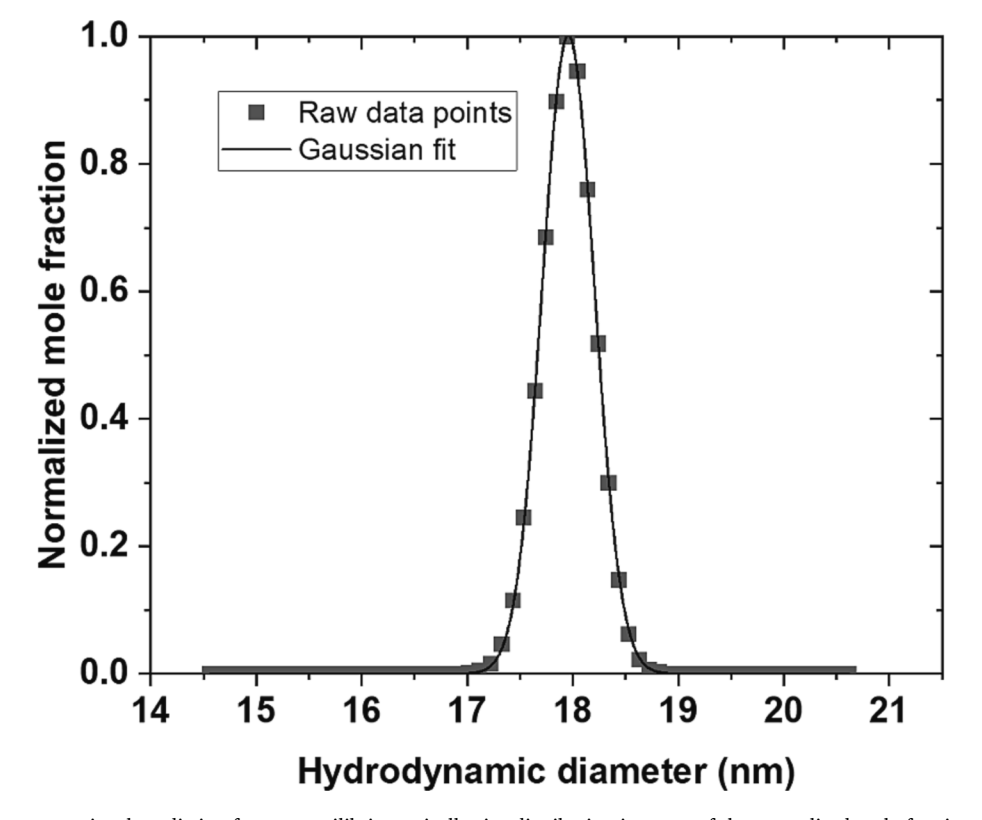
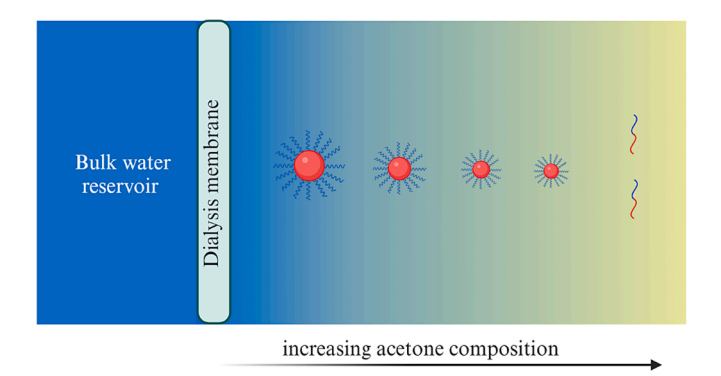


Fig. 4. Raw data of the computational prediction for non-equilibrium micelle size distribution in terms of the normalized mole fraction of micelles fitted with a Gaussian distribution for the 35% acetone/65% water ENP formulation condition.



**Fig. 5.** Schematic of the solvent profile during the solvent exchange (direct dialysis) procedure. This figure is reproduced in color on the web and in black-and-white in print.

results. First, the absolute magnitude of the mean  $D_h$  differ by about a factor of two. However, the relative change in diameter as a result of the formulation condition shows good agreement. For example, the experimental results show that the  $D_h$  increases from 28.1 nm to 32.8 nm when the formulation solvent conditions were changed from  $\Phi_{acetone} =$ 0.80 to  $\Phi_{acetone} = 0.50$  which is a 14 % increase in size. For the computational study, the  $D_h$  increases from 16.0 nm to 18.0 nm when solvent conditions were changed from  $\Phi_{acetone} = 0.80$  to  $\Phi_{acetone} = 0.50$ which represents at 11 % increase in size. Therefore, although the magnitude of the  $D_h$  values does not match precisely between the experimental and computational results, the magnitude of the change in size due to changing solvent conditions is captured well by the model. Next, by approximating each distribution with a gaussian distribution, the mean, standard deviation (SD), and coefficient of variance (CV) are extracted and are shown in Table 2 along with the corresponding experimental values. The CV (CV = SD/mean) is commonly used as a

measure of dispersity for nanoparticle systems. The theoretical calculations result in an extremely narrow distributions, CV < 0.02, for all the ENP cases. Because the quantity  $(\Delta \mu_{gj}^0 - \Delta \mu_{gj,e}^0)/kT$  in Eq. (S15) is large (estimated to vary around -40 - -30 as a function of g for standard parameters), any deviations from the most preferred aggregation number g (on the order of  $10^2$ ) will cause a large increase in the overall free energy in micellization  $g(\Delta \mu_{gi}^0 - \Delta \mu_{gi,e}^0)/kT$  in Eq. (S15). The CVs from the theoretical ENP size distributions are much lower than that measured using the DLS cumulant analysis; however, some of the ENP DLS size histograms do reflect the narrow distributions found using the modelling approach. The modelling results demonstrate that at equilibrium, the micelles should form an extremely uniform size population, and therefore should fall well below the monodisperse cutoff for DLS ( $CV = PDI^{1/2}$  $=0.1^{1/2}=0.316$ ). Although the experimental ENP method can produce CVs well below this cutoff, it is not able to achieve the extremely low CVs predicted by the modelling study. The reason for the discrepancy between the experimental and modelling results is likely because in the experimental case the acetone cannot be moved instantaneously which is the assumption in the modelling study. Therefore, there is some rearrangement which can occur in the experimental study which is not accounted for in the modelling study such that experimental size distributions do not represent the true equilibrium distributions.

The theoretical predictions also provide interesting results with regards to the effect of formulation method on the final size distribution. The theoretical results suggest the direct dialysis will have a significantly greater CV than any ENP formulation conditions. The experimental results reflect this finding for  $\Phi_{acetone}$  values less than 0.80, although the magnitude of difference is smaller in the experimental study. This suggests that ENP cases with high (> 0.80)  $\Phi_{acetone}$  formulation conditions are not ideal for the ENP procedure. However, in the range of  $\Phi_{acetone} = 0.70 - 0.50$ , ENP is much more effective at producing low dispersity as suggested by both experimental and theoretical results. The theoretical results also suggest that direct dialysis will produce a  $D_h$ 

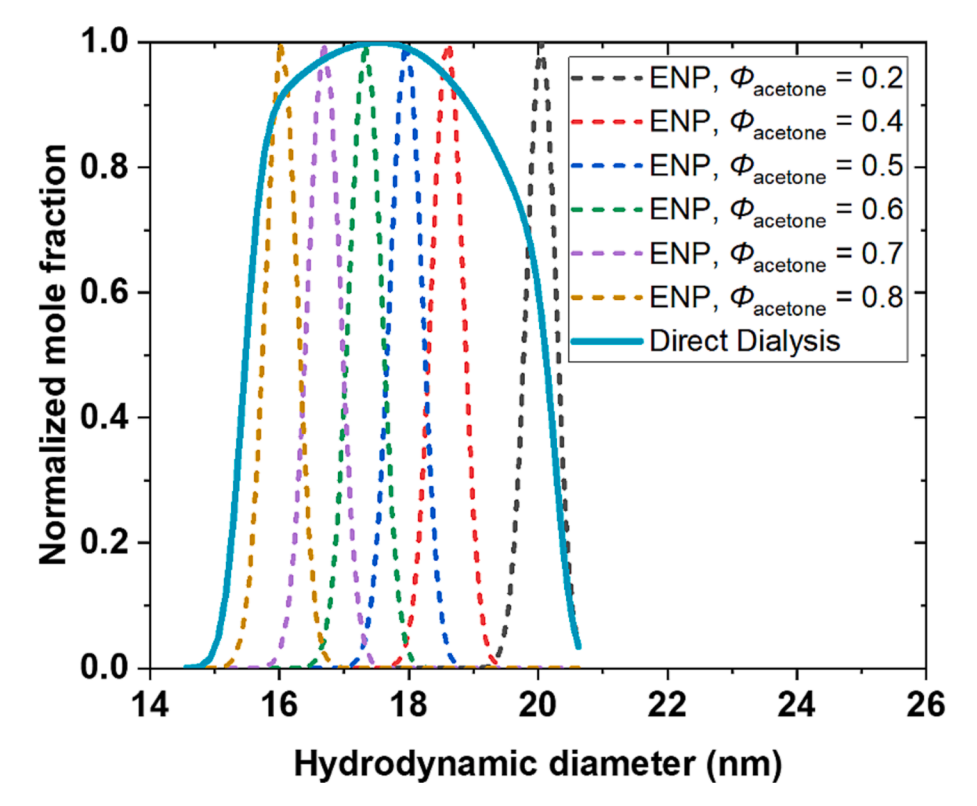


Fig. 6. Calculated size distributions after acetone removal for different ENP formulation conditions, labeled with the volume fraction of acetone at which micelles were formed, along with distribution from direct dialysis using the linear solvent profile assumption. This figure is reproduced in color on the web and in black-and-white in print.

nearly equivalent to the ENP case with  $\Phi_{acetone}=0.60$ . In the experimental results, the direct dialysis method produced a  $D_h$  which was closest to the ENP case with  $\Phi_{acetone}=0.50$ , which agrees reasonably well with the theoretical prediction. The DLS experimental size histograms for direct dialysis and some ENP cases indicate the presence of some larger aggregates (> 40 nm) which are not present in the theoretical size contributions. These large aggregates would serve to inflate by the  $D_h$  and PDI of the experimental results and can also help explain some of the discrepancy between the experimental and theoretical results. Also, for a more accurate modeling of the size distribution behavior for the direct dialysis process, it is essential to obtain quantitative information about the spatial solvent composition profile changes over time, especially near the dialysis membrane boundary. We plan to investigate this aspect in future research endeavors.

#### 4. Conclusions

The use of polymer nanoparticles in such applications as nanomedicine requires formulation methods which can effectively limit the size dispersity of the nanoparticles [26]. This study highlights how the Equilibration-Nanoprecipitation (ENP) method, designed to initiate micellization under uniform solvent conditions and equilibrate before organic co-solvent removal, shows superior control over micelle size and dispersity compared to a conventional solvent method which initiates self-assembly under a solvent gradient. Although previous experimental and modelling studies have highlighted the effect of water/co-solvent composition on the preferred aggregation number of polymer micelles [8,14,27], this study highlights for the first time the ability of using equilibrium self-assembly prior to co-solvent removal to limit the final dispersity of the non-equilibrium micelles in water. The modelling study indicates the overall free energy of micellization is very sensitive to even small changes in the aggregation number such that the distribution of sizes is very narrow at a given equilibrium solvent condition. Although the experimental ENP method cannot replicate the same magnitude of CV as the modelling study, it does demonstrate the ability to produce final non-equilibrium micelles with CVs below the DLS "monodisperse" threshold ( $PDI_{DLS} < 0.1$ ). The conventional solvent exchange method fails to achieve the same level of dispersity compared to ENP, and the relative increase is consistent with the modelling results. The PDI<sub>DLS</sub> values for other polymer nanoparticle systems using alternative formulation methods are commonly reported in the literature to be above this monodisperse threshold [28-33]. Therefore, the ENP method can serve as a straightforward approach for researchers looking to reduce the dispersity of the nanoparticle dispersions. In the future, the ENP method will be extended to demonstrate its utility in the encapsulation of hydrophobic compounds in the core domain of micelles as this is relevant for drug delivery and imaging applications.

### CRediT authorship contribution statement

**Daniel J. Fesenmeier:** Writing – original draft, Visualization, Methodology, Investigation, Formal analysis, Data curation, Conceptualization. **Elliot S. Cooper:** Writing – original draft, Visualization, Software, Methodology, Investigation, Data curation. **You-Yeon Won:** Writing – review & editing, Supervision, Resources, Project administration, Investigation, Funding acquisition, Conceptualization.

#### Declaration of competing interest

The authors declare that they have no known competing financial interests or personal relationships that could have appeared to influence the work reported in this paper.

# Data availability

Data will be made available on request.

#### Acknowledgements

The authors are grateful for funding from NSF (CBET-2211843). The authors also acknowledge support from the Purdue University Institute for Cancer Research (PU-ICR) via an NIH NCI grant (P30 CA023168), which supports the campus-wide NMR shared resources that were utilized in this work. The authors acknowledge that the Graphical Abstract, Fig. 1, and Fig. 5 were created with Biorender.com.

#### Appendix A. Supplementary data

Supplementary data to this article can be found online at https://doi.org/10.1016/j.jcis.2024.01.167.

#### References

- P. Alexandridis, B. Lindman. Amphiphilic block copolymers: self-assembly and applications, Elsevier, 2000.
- [2] G. Wanka, H. Hoffmann, W. Ulbricht, Phase diagrams and aggregation behavior of poly(oxyethylene)-poly(oxypropylene)-poly(oxyethylene) triblock copolymers in aqueous solutions, Macromolecules 27 (15) (1994) 4145–4159.
- [3] P. Alexandridis, T. Alan Hatton, Poly(ethylene oxide)-poly(propylene oxide)-poly (ethylene oxide) block copolymer surfactants in aqueous solutions and at interfaces: thermodynamics, structure, dynamics, and modeling, Colloids Surf. A Physicochem. Eng. Asp. 96 (1) (1995) 1–46.
- [4] M.Y. Kozlov, N.S. Melik-Nubarov, E.V. Batrakova, A.V. Kabanov, Relationship between pluronic block copolymer structure, critical micellization concentration and partitioning coefficients of low molecular mass solutes, Macromolecules 33 (9) (2000) 3305–3313.
- [5] Y. Yu, A. Eisenberg, Control of morphology through polymer–solvent interactions in crew-cut aggregates of amphiphilic block copolymers, J. Am. Chem. Soc. 119 (35) (1997) 8383–8384.
- [6] L. Zhang, K. Yu, A. Eisenberg, Ion-induced morphological changes in "crew-cut" aggregates of amphiphilic block copolymers, Science 272 (5269) (1996) 1777–1779.
- [7] P. Munk, Equilibrium and Nonequilibrium Polymer Micelles, in: S.E. Webber, P. Munk, Z. Tuzar (Eds.), Solvents and Self-Organization of Polymers, Springer, Netherlands, Dordrecht, 1996, pp. 19–32.
- [8] R. Nagarajan, "Non-equilibrium" block copolymer micelles with glassy cores: a predictive approach based on theory of equilibrium micelles, J. Colloid Interface Sci. 449 (2015) 416–427.
- [9] T. Nicolai, O. Colombani, C. Chassenieux, Dynamic polymeric micelles versus frozen nanoparticles formed by block copolymers, Soft Matter 6 (14) (2010) 3111–3118.
- [10] R. Nagarajan, Solubilization of hydrocarbons and resulting aggregate shape transitions in aqueous solutions of Pluronic® (PEO-PPO-PEO) block copolymers, Colloids Surf. B Biointerfaces 16 (1) (1999) 55–72.
- [11] R. Nagarajan, K. Ganesh, Comparison of solubilization of hydrocarbons in (PEO-PPO) diblock versus (PEO-PPO-PEO) triblock copolymer micelles, J. Colloid Interface Sci. 184 (2) (1996) 489–499.
- [12] L. Zhang, A. Eisenberg, Multiple morphologies of "crew-cut" aggregates of polystyrene-<i>b</i>-poly(acrylic acid) block copolymers, Science 268 (5218) (1995) 1728–1731.
- [13] L. Zhang, A. Eisenberg, Thermodynamic vs kinetic aspects in the formation and morphological transitions of crew-cut aggregates produced by self-assembly of polystyrene-b-poly(acrylic acid) block copolymers in dilute solution, Macromolecules 32 (7) (1999) 2239–2249.
- [14] R. Nagarajan, "Frozen" Micelles: Polymer Nanoparticles of Controlled Size by Self-Assembly, In Nanoparticles: Synthesis, Stabilization, Passivation, and Functionalization, ACS Symposium Series, American Chemical Society 996 (2008) 341, 356
- [15] Y.-Y. Won, D.J. Fesenmeier, Formulation of Monodisperse Kinetically Frozen Polymer Micelles via Equilibration-Nanoprecipitation. US Patent Application No. 17926105
- [16] D.J. Fesenmeier, S. Park, S. Kim, Y.-Y. Won, Surface mechanical behavior of water-spread poly(styrene)–poly(ethylene glycol) (PS–PEG) micelles at the air–water interface: effect of micelle size and polymer end/linking group chemistry, J. Colloid Interface Sci. 617 (2022) 764–777.
- [17] D.J. Fesenmeier, M.V. Suresh, S. Kim, S. Park, K. Raghavendran, Y.-Y. Won, Polymer lung surfactants attenuate direct lung injury in mice, ACS Biomater Sci. Eng. 9 (5) (2023) 2716–2730.
- [18] H.C. Kim, M.V. Suresh, V.V. Singh, D.Q. Arick, D.A. Machado-Aranda, K. Raghavendran, Y.-Y. Won, Polymer Lung Surfactants, ACS Appl. Bio Mater. 1 (3) (2018) 581–592.
- [19] S. Kim, D.J. Fesenmeier, S. Park, S.E. Torregrosa-Allen, B.D. Elzey, Y.-Y. Won, Pulmonary pharmacokinetics of polymer lung surfactants following pharyngeal administration in mice, Biomacromolecules 23 (6) (2022) 2471–2484.
- [20] S. Kim, S. Park, D.J. Fesenmeier, T. Jun, K. Sarkar, Y.-Y. Won, Surface pressurearea mechanics of water-spread poly(ethylene glycol)-based block copolymer micelle monolayers at the air-water interface: effect of hydrophobic block chemistry, Langmuir 39 (38) (2023) 13546–13559.

- [21] Y.Y. Won, H.T. Davis, F.S. Bates, Molecular exchange in PEO-PB micelles in water, Macromolecules 36 (3) (2003) 953–955.
- [22] H.C. Kim, D.Q. Arick, Y.Y. Won, Air-water interfacial properties of chloroform-spread versus water-spread poly((D, L-lactic acid-co-glycolic acid)-block-ethylene glycol) (PLGA-PEG) polymers, Langmuir 34 (16) (2018) 4874–4887.
- [23] S. Kim, M. Lee, H.C. Kim, Y. Kim, W.B. Lee, Y.-Y. Won, Determination of gass transition temperatures in bulk and micellar nanoconfined polymers by using fluorescent molecular rotors as probes for changes in free volume, Macromolecules 56 (16) (2023) 6290–6304.
- [24] D.J. Fesenmeier, H.C. Kim, S. Kim, Y.-Y. Won, Determination of block copolymer micelle core Tg using 1H NMR transverse (T2) relaxation measurements of micelle coronas, Macromolecules 56 (22) (2023) 9156–9163.
- [25] D.J. Fesenmeier, S. Kim, Y.-Y. Won, Effect of temperature on the air-water surface mechanical behavior of water-spread block copolymer micelles, Soft Matter 19 (2023) 9269–9281.
- [26] M. Danaei, M. Dehghankhold, S. Ataei, F. Hasanzadeh Davarani, R. Javanmard, A. Dokhani, S. Khorasani, M.R. Mozafari, Impact of particle size and polydispersity index on the clinical applications of lipidic nanocarrier systems, Pharmaceutics 10 (2) (2018) 57.
- [27] P. Alexandridis, L. Yang, SANS investigation of polyether block copolymer micelle structure in mixed solvents of water and formamide, ethanol, or glycerol, Macromolecules 33 (15) (2000) 5574–5587.

- [28] R. Ghasemi, M. Abdollahi, E. Emamgholi Zadeh, K. Khodabakhshi, A. Badeli, H. Bagheri, S. Hosseinkhani, mPEG-PLA and PLA-PEG-PLA nanoparticles as new carriers for delivery of recombinant human Growth Hormone (rhGH), Sci. Rep. 8 (1) (2018) 9854.
- [29] A. Salimi, B. Sharif Makhmal Zadeh, M. Kazemi, Preparation and optimization of polymeric micelles as an oral drug delivery system for deferoxamine mesylate: in vitro and ex vivo studies, Res. Pharm. Sci. 14 (4) (2019) 293–307.
- [30] J. Cheng, B.A. Teply, I. Sherifi, J. Sung, G. Luther, F.X. Gu, E. Levy-Nissenbaum, A. F. Radovic-Moreno, R. Langer, O.C. Farokhzad, Formulation of functionalized PLGA–PEG nanoparticles for in vivo targeted drug delivery, Biomaterials 28 (5) (2007) 869–876.
- [31] L. Shi, J. Shan, Y. Ju, P. Aikens, R.K. Prud'homme, Nanoparticles as delivery vehicles for sunscreen agents, Colloids Surf. A Physicochem. Eng. Asp. 396 (2012) 122–129.
- [32] A. Albisa, E. Piacentini, V. Sebastian, M. Arruebo, J. Santamaria, L. Giorno, Preparation of drug-loaded PLGA-PEG nanoparticles by membrane-assisted nanoprecipitation, Pharm. Res. 34 (6) (2017) 1296–1308.
- [33] S. Hornig, T. Heinze, C.R. Becer, U.S. Schubert, Synthetic polymeric nanoparticles by nanoprecipitation, J. Mater. Chem. 19 (23) (2009) 3838–3840.